Hindawi
Journal of Chemistry
Volume 2019, Article ID 2078360, 9 pages
https://doi.org/10.1155/2019/2078360

Research Article

CH_4/N_2 Adsorptive Separation on Zeolite X/AC Composites

Cai Long Xue, Wen Ping Cheng, Wen Ming Hao, Jing Hong Ma, and Rui Feng Li

College of Chemistry and Chemical Engineering, Taiyuan University of Technology, Taiyuan 030024, China

Correspondence should be addressed to Wen Ping Cheng; tycwp@163.com and Jing Hong Ma; majinghong@tyut.edu.cn

Received 26 September 2018; Accepted 21 November 2018; Published 2 January 2019

Academic Editor: Philippe Trens

A series of zeolite X/activated carbon (AC) composites were prepared from the same starting materials at various activation time. The corresponding modified samples were obtained by being treated with diluted NH_4Cl solution. The relationship between porosity development, surface properties, and CH_4/N_2 adsorption performance was investigated. The increase of micropore volume is beneficial to the improvement of CH_4 and N_2 adsorption capacity, but more sensitive for CH_4. In addition, the polar functional groups of zeolite X/AC composites may enhance CH_4 adsorption capacity. More importantly, both developing micropore structure and surface modification contributed to enhance the adsorption selectivity α_{CH_4/N_2}. As the optimum sample of these studies, HZAC(24) showed CH_4 adsorption capacity of 17.3 cm^3/g and the highest adsorption selectivity α_{CH_4/N_2} of 3.4. The CH_4 and N_2 adsorption isotherms of all samples can be well fitted by the Langmuir–Freundlich model. HZAC(24) showed an excellent cyclability of adsorption/desorption of CH_4 with a neglectable capacity loss after subsequent cycles. Moreover, HZAC(24) displayed relatively rapid adsorption kinetics. These properties of zeolite X/AC composites are essential for the adsorptive separation of CH_4 from N_2 in the pressure swing adsorption (PSA) process.

1. Introduction

The coal bed methane (CBM) is an unconventional gas with a main composition of CH_4, N_2, and CO_2, which reserve is about two times higher than that known to natural gas [1]. Nowadays, due to the CH_4 content in the drainage gas of coal mine is only 20–45%, CBM is usually extracted into the atmosphere, which not only is a waste of energy source but also pollutes the environment as CH_4 is one of the major contributors to the global warming with 20 times higher global warming potential than that of CO_2 [2, 3]. So, it is of great significance to develop and utilize the CBM. The content of CH_4 higher than 80% is required for the application of chemical raw stock and 90% for merging into the civil gas system [4]. For pipeline quality natural gas, the impurities of N_2 and CO_2 content should not exceed 4% and 2%, respectively [5, 6]. So, CH_4 separation from N_2 and CO_2 is one of the important industrial separation processes [7, 8]. However, CH_4 and N_2 possess extremely similar physicochemical properties and kinetic diameter. Therefore, it is a really large challenge to enrich CH_4 from the mixture of CH_4 and N_2 such as CBM.

Generally, membrane [9], cryogenic [10, 11], and adsorption separation [12] are applied to separate the CH_4 and N_2 mixture. Membrane separation has the drawbacks of low selectivity and the strongly dependence of the membrane which is liable to damage and block; thus, it is not economical in scale separation [13, 14]. Cryogenic separation requires high-energy consumption and is helpless for low flow rates. In comparison with other methods, adsorption separation with easy operation, lower energy requirement, lower operational cost, running continuous at ambient temperature, and so on attracts increasingly attention. During the past three decades, there has been a rapid growth in the development of adsorption-based technologies for separation and purification of different gas mixtures, so that it can be applied to medium-scale CH_4/N_2 separation. However, it is still a big challenge as for the larger-scale CH_4/N_2 adsorption separation due to the lack of satisfactory adsorbent with high adsorption capacity and selectivity.

Many materials have been developed for gas selective separation. Zeolites, as one of the candidates for enriching CH_4 from gas mixture, have shown great prospect and can potentially be used in the pressure swing adsorption (PSA) process. In order to obtain an appropriate zeolite for gas adsorption separation, the effect factors, including the pore structure of zeolite and the strength of the electric fields

caused by the presence of exchangeable cations in the frameworks, have been investigated [5, 14]. It has been found that zeolite X [15–21] is one of the most suitable zeolite adsorbents for adsorption and separation due to its large pore diameter of 0.74 nm which can accommodate large molecules and low Si/Al ratio with the presence of extra framework of cations that produces electric field which interacts strongly with the high polarizability CH_4 molecule or quadrupolar CO_2 molecules. Activated carbon [22–24], another promising candidate for gas separation, possesses lots of advantages such as tunable pore size, easy regeneration, and low cost. In general, activated carbons have higher equilibrium selectivity for CH_4 over N_2 but smaller adsorption capacities for CH_4 than zeolites. As a consequence, in order to integrate the advantages of both zeolite and activated carbon in industrial application, increasingly attentions have been concentrated on the synthesis of the novel porous material of zeolite/AC composites in recent years [25, 26]. Meanwhile, the environmental application such as wastewater treatment as well as gas separation using of zeolite/AC composites has been explored preliminarily [27, 28]. In our previous work, the zeolite X/AC composites from elutrilithe are prepared by adding pitch powder and precipitate silicon dioxide as an additional carbonaceous and silica source, respectively [25, 29, 30].

The main aim in this work is to introduce amine modifications in a series of zeolite X/AC composites with different activation time in order to increase the interactions with CH_4 without improving those with gases. This strategy will improve the potential of these materials to separate CH_4/N_2 mixtures, making these materials candidates for natural gas upgrading. The effect of pore texture and surface properties of the adsorbents on the adsorption performance of CH_4 and N_2 was investigated in detail.

2. Experimental

2.1. Preparation of Zeolite X/AC Composites. Zeolite X/AC composites were prepared by the following two steps. First, the locally available Elutrilithe chunk, with major chemical composition of 41.0 wt.% SiO_2, 35.5 wt.% Al_2O_3, and 7.0 wt.% C, was crashed and sieved in order to collect the grains with an average size below 200 meshes. The elutrilithe powder was then simply physically mixed with precipitated silica (ca.93% SiO_2) and pitch powder in order to get a constant molecular ratio $SiO_2/Al_2O_3 = 4.5$ and a final mass composition of 50 wt.% carbon. The obtained blend powder was kneaded with defined amount of deionized water and extruded into a cylinder shape with dimensions of φ2.0 mm × 6.0 mm by extruder. After drying overnight, the extrudates were calcined in a tubular furnace under a stream of N_2 with a flow rate of 150 ml/min at 723 K for 2 h and following 1123 K for 2 h. After that, the temperature of 1123 K was maintained for time t_a, and the atmosphere was switched from N_2 to CO_2 (200 ml/min) for activation. t_a is a variable activation parameter, ranging from 4 h to 32 h. A heating rate of 5 K/min was applied up to the appointed temperature in the above procedure. Subsequently, the activated samples were treated with a NaOH hydrothermal system in a flash ($Al_2O_3 : SiO_2 : Na_2O : H_2O = 1 : 4.5 : 4.5 : 135$), and then, the products were filtered, washed with deionized water at 323–343 K until the pH of the products reached around 7, and dried at 373 K for at least 6 h. ZAC(t_a) (t_a = 4, 16, 24, and 32, which represent the activation time of 4 h, 16 h, 24 h, and 32 h) is used to mark the composites, and the corresponding burn-off of ZAC(t_a) is 42, 29, 21, and 17%, respectively.

The surface modification of the composites was carried out by the conventional soaking method. A typical soaking method involved adding 250 mL of 0.3 mol/L NH_4Cl solution to about 10 g composite. The solution was heated to 340 K for 0.5 h. After that, the solution was decanted, and fresh solution was added. This procedure was repeated three times. After modification, the samples were filtered and washed with copious amount of deionized water until the effluent was free from chloride ions as tested with $AgNO_3$ solution. The resulting products were dried at 373 K for more than 6 h and calcined in a tube furnace at 623 K for 2 h under vacuum to dislodge the NH_3 in the products. The corresponding products after modification were denoted as HZAC(t_a) (t_a = 4, 16, 24, and 32, which represent the activation time of 4 h, 16 h, 24 h, and 32 h).

2.2. Characterization. X-ray powder diffraction (XRD) patterns of the materials were obtained using a Shimadzu LabX XRD-6000 system in the 2θ range of 5–35° using CuKα1 (λ = 1.54056 Å) radiation operated with 40 kV and 30 mA. The surface area and pore volume of the products were calculated from N_2 adsorption isotherms measured on a surface area and pore size analyzer, QUADRASORB SI, (Quantachrome Inc., USA) after degassing the samples at 623 K for at least 4 h under high vacuum. The surface areas (S_{BET}) were calculated by using the Brunauer–Emmett–Teller (BET) equation at the relative pressure in the range of 0.01–0.2. The micropore volume (V_{mic}) and micropore surface (S_{mic}) area were determined by the t-plot method. The amount of N_2 absorbed at $P/P_0 = 0.98$ was employed to calculate the total pore volume (V_{total}). The total basicity of the samples was determined by temperature-programmed desorption of carbon dioxide (CO_2-TPD) using a type of TP-5076 TPR/TPD automatic temperature-programmed chemical adsorption apparatus. The surface properties of the samples were analyzed by employing a conventional Boehm titration procedure. Aqueous solutions of NaOH, HCl, Na_2CO_3, and $NaHCO_3$ (0.1 mol/L) with the volume of 25 mL were decanted into conical flasks with 1 g sample each, respectively, and after shaking for 1 h, the conical flasks were kept standing for 48 h, and then filtered. The filtrates were diluted and employed back titration with standard solution to calculate the amount of surface function groups on the samples.

2.3. Adsorption Measurements. The presence of water in the composites significantly affects the adsorption isotherm; therefore, all the samples were calcined at 573 K for 4 h under N_2-flow in a tubular furnace. Prior to adsorption measurements, the samples were degassed under vacuum by heating up to 623 K for at least 4 h. The CH_4 and N_2

adsorption isotherms were measured at 273 K using a static volumetric apparatus of NOVE1200e instrument (Quantachrome Inc., USA). The adsorption kinetics curve was measured by releasing a small amount of CO_2 with the type NOVE1000e instrument (Quantachrome Inc., USA). During the adsorption, measurement temperature was maintained by circulating ethanediol-water from a constant temperature bath. The adsorption capacity was determined from the adsorption isotherm measured at 273 K, and the pure component selectivity of CH_4 and N_2 (α_{CH_4/N_2}) was calculated by using the following equation:

$$\alpha_{CH_4/N_2} = \left[\frac{V_{CH_4}}{V_{N_2}}\right]_{P,T}, \quad (1)$$

where V_{CH_4} and V_{N_2} are the adsorption amount (at 273 K, 100 kPa) of CH_4 and N_2, respectively.

3. Results and Discussion

3.1. Zeolite X/AC Composites. The XRD patterns of zeolite X/AC composites before and after modification are shown in Figure 1. It can be seen that all samples are highly crystalline materials giving the reflections in the range of 5–35° and exhibit characteristic peaks of zeolite X without other impurity phases. The crystallinity of zeolite X decreases after surface modification as evidenced from the decrease of the intensity of the major characteristic peaks of zeolite X. This is due to the partially collapse of the crystalline structure, which is consistent with the conclusion from others [31, 32].

Figure 2 displays N_2 adsorption-desorption isotherms at 77 K on a series of samples. All isotherms exhibit the characteristic combination of the type-I and type-IV morphology, indicating the coexistence of micropores and mesopores in the composites [33]. Table 1 summarizes their pore structure parameters calculated from the isotherms. It can be seen that, as far as $t_a \leq 24$ h, the S_{BET}, S_{mic}, V_{total}, and V_{mic} of ZAC(t_a) samples presented a significant rising trend, and it occurred sharply decrease thereafter, while the S_{ext} was increasing with lengthening the activated time. This means that extending the activation time when $t_a \leq 24$ h mainly induces the creation of new pores, while widening of pores becomes the main mechanism of porosity development with longer activation time [25]. In addition, the treatment of NH_4Cl solution has a significant effect on the textual properties. In comparison with ZAC(t_a), the pore structure parameters of HZAC(t_a) decrease except S_{ext}, due to the partially collapse of the crystalline structure in the composites during surface modification [32].

The CO_2-TPD results of ZAC(t_a) and HZAC(t_a) are shown in Figure 3. For ZAC(t_a) samples, a larger desorption peak at 573–673 K and a little shoulder peak take place at around 383 K, corresponding to the surface basic site; however, there is only one desorption peak of HZAC(t_a) samples at about 473–573 K. From Figure 3, it can be seen that CO_2 desorption peak areas increase and CO_2 desorption peak moves to higher temperature for ZAC(t_a) samples when increasing activation time, indicating that the amount and strength of surface basic groups rising, respectively. The variation tendency of the surface basic properties of HZAC(t_a) is similar with ZAC(t_a). However, both the amount of the surface basic groups and basic strength decline for HZAC(t_a) compared with ZAC(t_a), which resulted from the treatment by NH_4Cl solution. In addition, Figure 4 shows the representative Boehm titration results of ZAC(24) and HZAC(24), which shows that the basic groups decrease almost half, and phenolic, carboxylic, and the total acidic groups sharply increase. These results are similar to the reports from references [34–36].

3.2. CH_4 and N_2 Adsorption Isotherms. The pure component CH_4 and N_2 adsorption isotherms at 273 K on the samples of ZAC(t_a) and HZAC(t_a) have been generated and are given in Figure 5. All curves are found to be type-I as per the IUPAC classification, and the low-pressure adsorption isotherms behave linearly [14, 33], which is ideal for sorbent regeneration, since most of the working capacity is recovered at moderate pressure ranges. A summary of adsorption and separation parameters extracted from adsorption isotherms is presented in Table 1. It can be seen that the CH_4 adsorption capacity is higher than that of N_2 on all of the samples. The CH_4 and N_2 adsorption capacity and CH_4/N_2 adsorption selectivity increased with the increase of V_{mic}. After the composites being treated by NH_4Cl, both of the CH_4 and N_2 adsorption capacity on the composites decreased; however, the CH_4/N_2 adsorption selectivity increased significantly.

Equilibrium adsorption isotherms in adsorbents are required for the available modeling or simulation of the various PSA separation processes of CH_4 and N_2 in practical application. Hence, in order to extend its utility, the collected experimental adsorption isotherm data should be fitted to an isotherm model [37]. In the present work, the adsorption isotherms of CH_4 and N_2 on all samples are fitted using the conventional Langmuir–Freundlich (L-F) (equation (2)) adsorption model [38, 39]:

$$Q = \frac{Q_m b_{L-F} p^{1/n}}{\left(1 + b_{L-F} p^{1/n}\right)}, \quad (2)$$

where p is the pressure, Q is the corresponding amount of the adsorbate adsorbed, Q_m is the saturation capacity of the adsorbent, b_{L-F} is the adsorption affinity defined by the van't Hoff equation for a heterogeneous solid, and n is the reciprocal of the Freundlich heterogeneity factor (the larger the value, the more the deviation from the Langmuir isotherm). Both b_{L-F} and n are empirical constants to be obtained by the data fitting method. Fitted parameters of the CH_4 and N_2 adsorption isotherms for all samples with L-F models are listed in Table 2. It can be seen that the Langmuir–Freundlich model is well correlated with the experimental adsorption data over the entire pressure range studied. Obviously, the values of b_{L-F} of CH_4 adsorption are higher than that of N_2 for ZAC(t_a), suggesting the stronger interaction between CH_4 and the samples than that between N_2 and the composites. After NH_4Cl treatment, the value of b_{L-F} decreases for N_2 adsorption, due to a decrease in the interaction between N_2 and modified composites. However,

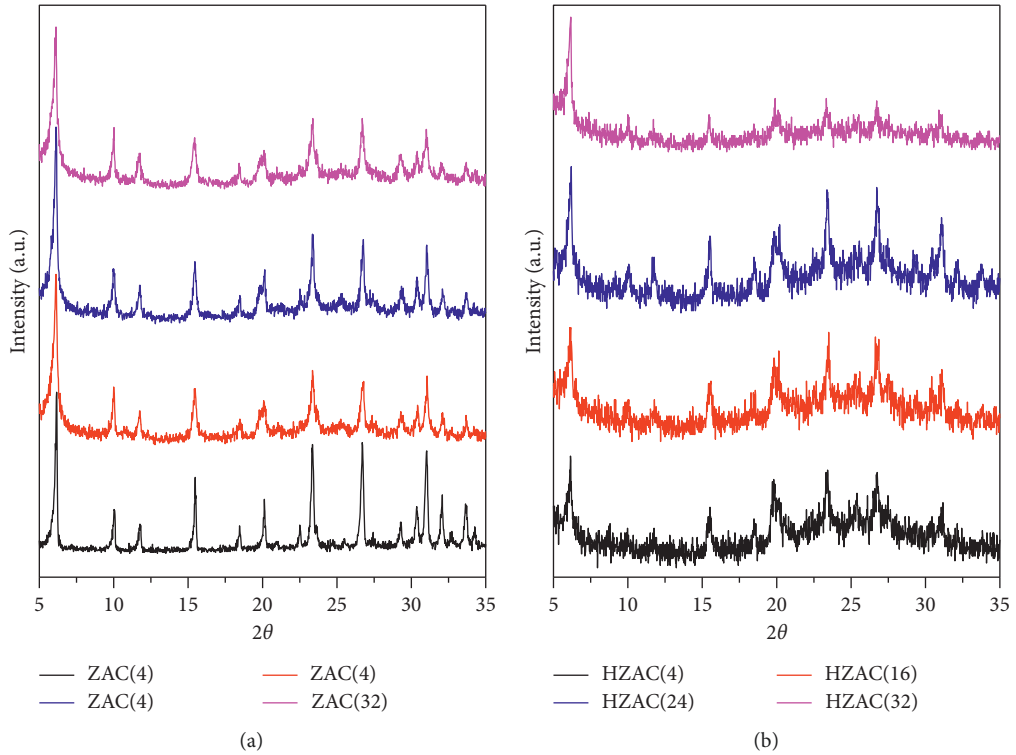

Figure 1: XRD patterns of ZAC(t_a) and HZAC(t_a).

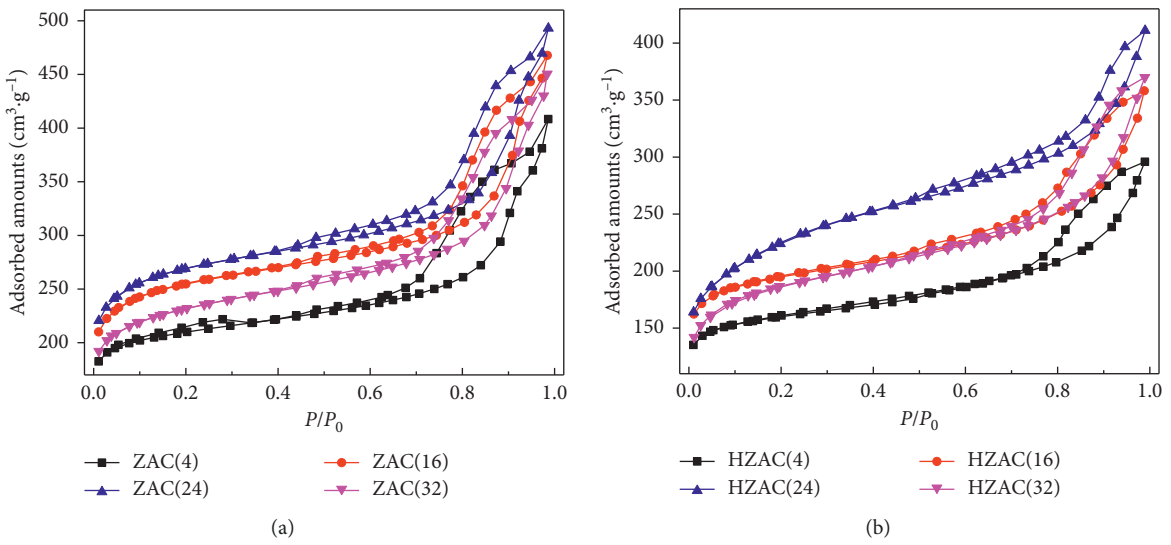

Figure 2: N_2 adsorption-desorption isotherms at 77 K of ZAC(t_a) and HZAC(t_a).

b_{L-F} increases for CH_4 adsorption, and the higher value of b_{L-F} for HZAC(t_a) is due to an increase in the interaction between CH_4 and HZAC(t_a). The changes in the b_{L-F} values of both CH_4 and N_2 adsorptions explain well the increase of the CH_4/N_2 selectivity on HZAC(t_a).

3.3. Effect of Pore Structure and Surface Properties on the Adsorption Performance. In order to improve the CH_4/N_2 adsorption selectivity and maintain the adsorption capacity of CH_4, the relationship between CH_4 and N_2 adsorption properties and the pore texture were studied in detail. ZAC(32) possesses a lower V_{mic} and a larger S_{ext} than ZAC(24), and the adsorption capacity and selectivity of CH_4 and N_2 showed the lower values on ZAC(32), indicating that the high adsorption capacity and selectivity of CH_4 and N_2 results from the large micropore volume rather than S_{ext} [40–45]. In Figure 6, the adsorption capacity of CH_4 and N_2 and adsorption selectivity α_{CH_4/N_2} are plotted versus V_{mic}. For ZAC(t_a), as the V_{mic} increased from 0.275 cm^3/g to

Table 1: Pore structure properties and CH_4/N_2 adsorptive separation performance of samples.

Samples	S_{BET} (m^2/g)	S_{mic} (m^2/g)	S_{ext} (m^2/g)	V_{mic} (cm^3/g)	V_{total} (cm^3/g)	Adsorption capacity (cm^3/g)		α
						CH_4	N_2	
ZAC(4)	816	694	121	0.275	0.633	16.1	7.52	2.1
ZAC(16)	965	828	136	0.341	0.725	19.1	8.37	2.3
ZAC(24)	1018	868	150	0.357	0.765	22.6	9.39	2.4
ZAC(32)	871	709	168	0.293	0.699	18.2	8.25	2.2
HZAC(4)	610	482	128	0.196	0.459	14.4	5.16	2.7
HZAC(16)	741	592	149	0.238	0.555	16.4	5.12	3.2
HZAC(24)	802	627	175	0.273	0.636	17.3	5.10	3.4
HZAC(32)	695	511	184	0.211	0.572	16.0	5.12	3.1

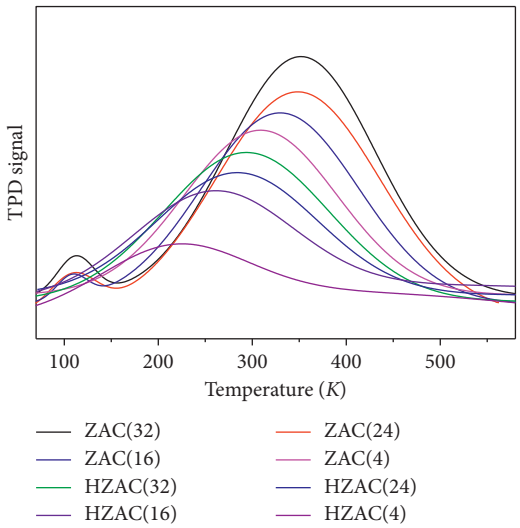

Figure 3: CO_2-TPD of ZAC(t_a) and HZAC(t_a).

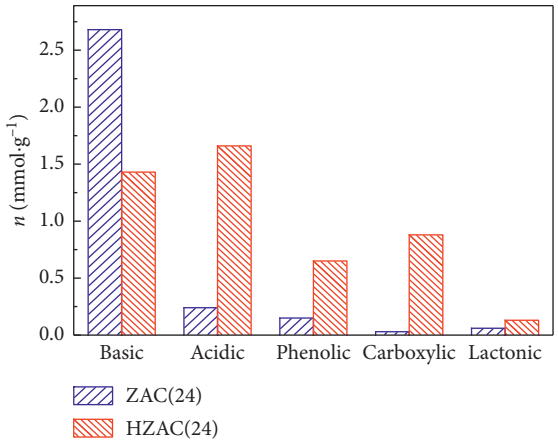

Figure 4: Results of Boehm titration on ZAC(24) and HZAC(24) samples.

0.357 cm^3/g, the adsorption capacity of CH_4 and N_2 increased from 16.1 cm^3/g to 22.6 cm^3/g and 7.52 cm^3/g to 9.39 cm^3/g, respectively. When the V_{mic} increases from 0.196 cm^3/g to 0.273 cm^3/g for HZAC(t_a), the CH_4 adsorption capacity increases from 14.4 cm^3/g to 17.3 cm^3/g. The adsorption selectivity α_{CH_4/N_2} for ZAC(t_a) and HZAC(t_a) presents a slight rise tendency. As a summary, with the increase of V_{mic}, CH_4 and N_2 adsorption capacity increased, and adsorption selectivity α_{CH_4/N_2} enhances slightly at the same time. However, the CH_4 and N_2 adsorption properties of ZAC(4) are different from HZAC(24) although the values of V_{mic} for the two samples are similar, which suggests that the pore structure is not the only factor affecting the gases adsorption performance on the samples.

Besides pore structure, the surface properties are also considered to be a significant factor on the gas adsorption process of the studied samples. After the treatment by NH_4Cl, the basic groups decreased severely and the acidic groups including phenolic and carboxylic groups sharply increased. Although CH_4 is a nonpolar molecule, it has a higher polarizability of 26×10^{-25} cm^3 [46]. Such polarizability causes a momentary shift in the time when the neutral electrostatic field of CH_4 is in close proximity to the larger polar function groups such as phenolic and carboxylic groups within the composites. The polarizability of N_2 (17.6×10^{-25} cm^3) is much lower than that of CH_4. Hence, the increasing of polar functional groups is more conducive to enhance the interaction between CH_4 molecule and the adsorbents [32, 39, 40, 47]. The reduction of the CH_4 adsorption capacity resulted from the decrease of V_{mic} in HZAC(t_a) was offset partially by the increase in interaction strongly between CH_4 molecule and HZAC(t_a). These characteristics lead to a moderate decrease in CH_4 adsorption capacity and a drastic decrease in N_2 adsorption capacity after NH_4Cl treatment; therefore, the adsorption selectivity α_{CH_4/N_2} on the HZAC(t_a) is extremely higher than that on the ZAC(t_a). In conclusion, there is a positive correlation between CH_4 adsorption capacity and adsorption selectivity α_{CH_4/N_2} and the V_{mic}. When the V_{mic} of samples is similar, the CH_4 adsorption capacity and the adsorption selectivity α_{CH_4/N_2} depended on the surface properties of the samples. HZAC(24) with a considerable V_{mic} and a higher amount of acidic groups has satisfactory CH_4 adsorption capacity and the maximum adsorption selectivity α_{CH_4/N_2} among the studied samples.

3.4. Cycle Adsorption and Time-Dependent Adsorption Capacity of CH_4. As adsorption-driven gas separation processes depend on the cyclic regeneration of the adsorbent,

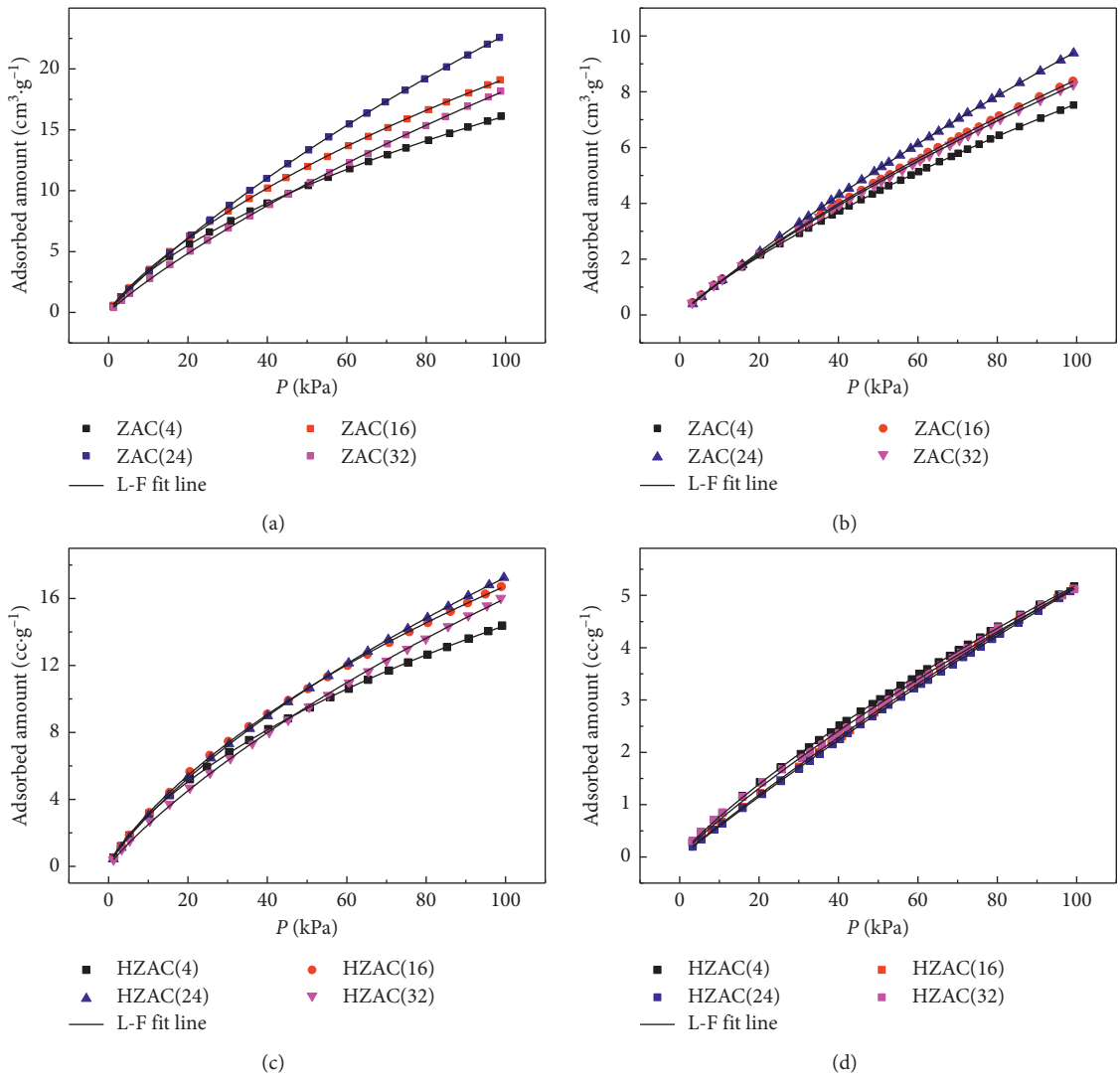

Figure 5: Adsorption isotherm of (a, c) CH_4 and (b, d) N_2 at 273 K on ZAC(t_a) and HZAC(t_a).

Table 2: L-F fitting parameters of CH_4 and N_2 isotherms on ZAC(t_a) and HZAC(t_a).

Adsorbate	Adsorbent	L-F model			
		Q_m (cm^3/g)	$b_{L\text{-}F} \times 10^{-3}$ (kPa^{-1})	n	R^2
N_2	ZAC(4)	48.6	3.3	1.14	0.999
	ZAC(16)	55.0	2.7	1.09	0.999
	ZAC(24)	57.4	2.2	1.02	0.999
	ZAC(32)	52.0	2.7	1.08	0.999
	HZAC(4)	38.5	2.6	1.13	0.999
	HZAC(16)	36.7	1.7	1.01	0.999
	HZAC(24)	40.1	1.5	1.00	0.999
	HZAC(32)	38.2	2.3	1.09	0.998
CH_4	ZAC(4)	64.6	8.7	1.27	0.999
	ZAC(16)	81.5	6.6	1.20	0.999
	ZAC(24)	105.6	3.8	1.17	0.999
	ZAC(32)	81.9	3.7	1.06	0.999
	HZAC(4)	53.4	10.0	1.28	0.999
	HZAC(16)	64.5	7.6	1.20	0.999
	HZAC(24)	86.0	5.3	1.19	0.999
	HZAC(32)	77.1	4.3	1.11	0.999

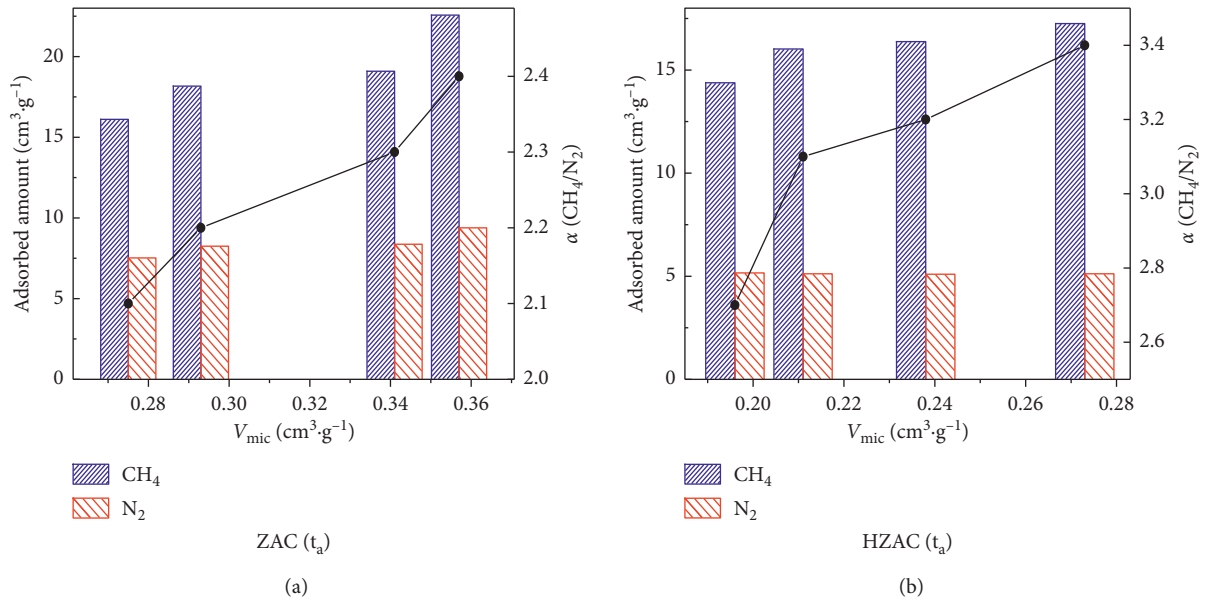

Figure 6: CH_4 and N_2 adsorption capacity and selectivity plotted of V_{mic}: (a) ZAC(t_a) and (b) HZAC(t_a).

it is important to study the cyclic adsorption performance of the adsorbents during long-term cyclical operation [48]. The successive adsorption/desorption cycles on HZAC(24) were carried out for nine times, and the results are shown in Figure 7. Within each cycle, the HZAC(24) was regenerated by reducing the pressure of CH_4 along the desorption branch and finally reached the conditions of a dynamic vacuum. The maximum CH_4 adsorbed amount was almost constant in nine cycles of adsorption and desorption, indicating that the CH_4 adsorption performance of HZAC(24) is stable. The results suggest that the zeolite X/AC composite can be easily regenerated by vacuum in the CH_4 adsorption system and be reused for many circles without any decay for the adsorption capacity.

For potential applications of zeolite X/AC composite in adsorption-driven separation of CH_4 from CH_4/N_2 mixture, it is also crucial that the adsorption of CH_4 is rapid. Typically, the industrial adsorption process is shorter than 1 min [49]. Here, we studied the time-dependent adsorption of CH_4 on HZAC(24) by releasing a small amount of CH_4 and studying the adsorbed amount as a function of time as shown in Figure 8. HZAC(24) displayed a relatively rapid adsorption kinetics, reaching 96% of the CH_4 capacity within 40 s. The rapid uptake indicates that zeolite X/AC composite can meet the requirements for an adsorbent used in the PSA process for the separation of CH_4.

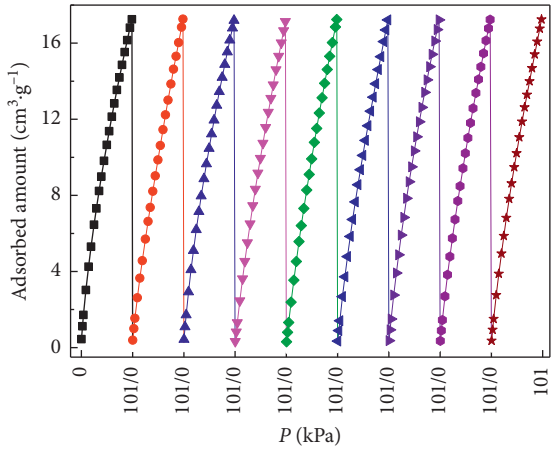

Figure 7: Adsorption and desorption cycles for CH_4 on HZAC(24).

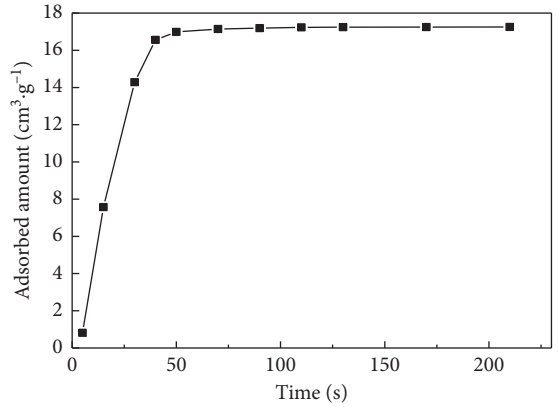

Figure 8: Uptake kinetics for HZAC(24) at 273 K.

4. Conclusions

Zeolite X/AC composites with different pore textures were prepared and then treated by diluted NH_4Cl solution. With the increase of activation time, the micropore volume increased, which reaches the maximum at the activation time of 24 hours. Furthermore, the increase of the micropore volume is beneficial to enhance the adsorption capacity of CH_4 and the adsorption selectivity α_{CH_4/N_2}. The increase of acidic oxygen-containing functional groups on sample surface significantly contributed to enhancing the adsorption selectivity α_{CH_4/N_2}, but leading to the decrease of the

adsorption capacity of CH_4. The HZAC(24) sample showed the highest adsorption selectivity α_{CH_4/N_2} of 3.4 among the studied samples and a high CH_4 adsorption capacity of 17.3 cm^3/g. The isotherms of CH_4 and N_2 on the composites before and after NH_4Cl treatment can be well fitted by the Langmuir–Freundlich model. Moreover, the HZAC(24) showed excellent cyclability of adsorption/desorption of CH_4 and relatively rapid adsorption kinetics. The present work provides a promising sight of applying zeolite X/AC composites from an economic and simple synthesis route as CH_4 adsorbent with high adsorption selectivity α_{CH_4/N_2}.

Data Availability

The data used to support the findings of this study are included within the article.

Conflicts of Interest

The authors declare that they have no conflicts of interest.

Acknowledgments

We gratefully appreciate the financial support from the National Natural Science Foundation of China (No. 51204120), Natural Science Foundation of Shanxi (No. 2014021014-1), and Key Scientific and Technological Project of Coal Fund of Shanxi province (No. FT201402-03).

References

[1] Q. Jiang, *Report on China Coal Bed Methane Industry for 2010–2015*, 2010, http://www.ocn.com.cn/reports/2006131meiceng.htm.

[2] C. A. Grande, F. V. S. Lopes, A. M. Ribeiro, J. M. Loureiro, and A. E. Rodrigues, "Adsorption of off-gases from steam methane reforming (H_2, CO_2, CH_4, CO and N_2) on activated carbon," *Separation Science and Technology*, vol. 43, no. 6, pp. 1338–1364, 2008.

[3] F. V. S. Lopes, C. A. Grande, A. M. Ribeiro, V. J. P. Vilar, J. M. Loureiro, and A. E. Rodrigues, "Effect of ion exchange on the adsorption of steam methane reforming off-gases on zeolite 13X," *Journal of Chemical & Engineering Data*, vol. 55, no. 1, pp. 184–195, 2010.

[4] Engelhard Corporation, *Adsorption Processes for Natural Gas Treatment, A Technology Update*, Engelhard Corporation, Newark, NY, USA, 2005, http://www.engelhard.com.

[5] R. S. Pillai, G. Sethia, and R. V. Jasra, "Sorption of CO, CH_4, and N_2 in alkali metal ion exchanged zeolite-X: grand canonical Monte Carlo simulation and volumetric measurements," *Industrial & Engineering Chemistry Research*, vol. 49, no. 12, pp. 5816–5825, 2010.

[6] R. T. Yang, "Gas Separation by Adsorption Processes," in *Chemical Engineering Science*, Vol. 43, Butterworth-Heinemann, Oxford, UK, 1997.

[7] A. Jayaraman, A. J. Hernandez-Maldonado, R. T. Yang, D. Chinn, C. L. Munson, and D. H. Mohr, "Clinoptilolites for nitrogen/methane separation," *Chemical Engineering Science*, vol. 59, no. 12, pp. 2407–2417, 2004.

[8] D. M. Ruthven, "Sorption of oxygen, nitrogen, carbon monoxide, methane, and binary mixtures of these gases in 5A molecular sieve," *AIChE Journal*, vol. 22, no. 4, pp. 753–759, 2010.

[9] P. Tremblay, M. Savard, J. Vermette, and R. Paquin, "Gas permeability, diffusivity and solubility of nitrogen, helium, methane, carbon dioxide and formaldehyde in dense polymeric membranes using a new on-line permeation apparatus," *Journal of Membrane Science*, vol. 282, no. 1-2, pp. 245–256, 2006.

[10] T. Gao, W. Lin, A. Gu, and M. Gu, "Coalbed methane liquefaction adopting a nitrogen expansion process with propane pre-cooling," *Applied Energy*, vol. 87, no. 7, pp. 2142–2147, 2010.

[11] W. S. Gao, X. S. Lu, W. S. Lin, and A. Z. Gu, "Parameter comparison of two small-scale natural gas liquefaction processes in skid-mounted packages," *Applied Thermal Engineering*, vol. 26, no. 8-9, pp. 898–904, 2005.

[12] R. T. Yang, *Adsorbents: Fundamentals and Applications*, John Wiley & Sons, Hoboken, NJ, USA, 2003.

[13] K. S. Knaebel and H. E. Reinhold, "Landfill gas: from rubbish to resource," *Adsorption*, vol. 9, no. 1, pp. 87–94, 2003.

[14] G. Sethia, R. S. Somani, and H. C. Bajaj, "Sorption of methane and nitrogen on cesium exchanged zeolite-X: structure, cation position and adsorption relationship," *Industrial & Engineering Chemistry Research*, vol. 53, no. 16, pp. 6807–6814, 2014.

[15] A. Arefi Pour, S. Sharifnia, R. NeishaboriSalehi, and M. Ghodrati, "Performance evaluation of clinoptilolite and 13X zeolites in CO_2 separation from CO_2/CH_4 mixture," *Journal of Natural Gas Science and Engineering*, vol. 26, pp. 1246–1253, 2015.

[16] F. Bandarchian and M. Anbia, "Conventional hydrothermal synthesis of nanoporous molecular sieve 13X for selective adsorption of trace amount of hydrogen sulfide from mixture with propane," *Journal of Natural Gas Science and Engineering*, vol. 26, pp. 1380–1387, 2015.

[17] V. Garshasbi, M. Jahangiri, and M. Anbia, "Equilibrium CO_2 adsorption on zeolite 13X prepared from natural clays," *Applied Surface Science*, vol. 393, pp. 225–233, 2017.

[18] P. Gómez-Álvarez, S. Hamad, M. Haranczyk, A. R. Ruiz-Salvador, and S. Calero, "Comparing gas separation performance between all known zeolites and their zeolitic imidazolate framework counterparts," *Dalton Transactions*, vol. 45, no. 1, pp. 216–225, 2016.

[19] Y. Qin, Z. Mo, W. Yu et al., "Adsorption behaviors of thiophene, benzene, and cyclohexene on FAU zeolites: comparison of CeY obtained by liquid-, and solid-state ion exchange," *Applied Surface Science*, vol. 292, no. 1, pp. 5–15, 2014.

[20] S. Salehi and M. Anbia, "Adsorption selectivity of CO_2 and CH_4 on novel PANI/Alkali-Exchanged FAU zeolite nanocomposites," *Journal of Inorganic and Organometallic Polymers and Materials*, vol. 27, no. 5, pp. 1281–1291, 2017.

[21] A. Villarreal, G. Garbarino, P. Riani et al., "Adsorption and separation of CO_2 from N_2-rich gas on zeolites: Na-X faujasite vs Na-mordenite," *Journal of CO_2 Utilization*, vol. 19, pp. 266–275, 2017.

[22] C. Liu, Y. Dang, Y. Zhou et al., "Effect of carbon pore structure on the CH_4/N_2 separation," *Adsorption*, vol. 18, no. 3-4, pp. 321–325, 2012.

[23] S. Y. Sawant, K. Munusamy, R. S. Somani, M. John, B. L. Newalkar, and H. C. Bajaj, "Precursor suitability and pilot scale production of super activated carbon for greenhouse gas adsorption and fuel gas storage," *Chemical Engineering Journal*, vol. 315, pp. 415–425, 2017.

[24] K. X. Yao, Y. Chen, Y. Lu, Y. Zhao, and Y. Ding, "Ultramicroporous carbon with extremely narrow pore distribution

and very high nitrogen doping for efficient methane mixture gases upgrading," *Carbon*, vol. 122, pp. 258–265, 2017.

[25] J. Ma, J. Tan, X. Du, and R. Li, "Effects of preparation parameters on the textural features of a granular zeolite/activated carbon composite material synthesized from elutrilithe and pitch," *Microporous and Mesoporous Materials*, vol. 132, no. 3, pp. 458–463, 2010.

[26] M. Miyake, Y. Kimura, T. Ohashi, and M. Matsuda, "Preparation of activated carbon-zeolite composite materials from coal fly ash," *Microporous and Mesoporous Materials*, vol. 112, no. 1–3, pp. 170–177, 2008.

[27] K. Y. Foo and B. H. Hameed, "The environmental applications of activated carbon/zeolite composite materials," *Advances in Colloid and Interface Science*, vol. 162, no. 1-2, pp. 22–28, 2011.

[28] V. K. Jha, M. Matsuda, and M. Miyake, "Sorption properties of the activated carbon-zeolite composite prepared from coal fly ash for Ni^{2+}, Cu^{2+}, Cd^{2+}, and Pb^{2+}," *Journal of Hazardous Materials*, vol. 160, no. 1, pp. 148–153, 2008.

[29] Z. Li, X. Cui, J. Ma, W. Chen, W. Gao, and R. Li, "Preparation of granular X-type zeolite/activated carbon composite from elutrilithe by adding pitch and solid SiO_2," *Materials Chemistry and Physics*, vol. 147, no. 3, pp. 1003–1008, 2014.

[30] J. Ma, H. Sun, S. Su, W. Cheng, and R. Li, "A novel double-function porous material: zeolite-activated carbon extrudates from elutrilithe," *Journal of Porous Materials*, vol. 15, no. 3, pp. 289–294, 2007.

[31] S. Lee, H. Kim, and M. Choi, "Controlled decationization of X zeolite: mesopore generation within zeolite crystallites for bulky molecular adsorption and transformation," *Journal of Materials Chemistry A*, vol. 1, no. 39, p. 12096, 2013.

[32] D. Zhang, W. Cheng, J. Ma, and R. Li, "Influence of activated carbon in zeolite X/activated carbon composites on CH_4/N_2 adsorption separation ability," *Adsorption*, vol. 22, no. 8, pp. 1129–1135, 2016.

[33] S. Brunauer, P. H. Emmett, and E. Teller, "Adsorption of gases in multimolecular layers," *Journal of the American Chemical Society*, vol. 60, no. 2, pp. 309–319, 1938.

[34] X. Lu, D. Jin, S. Wei et al., "Competitive adsorption of a binary CO_2-CH_4 mixture in nanoporous carbons: effects of edge-functionalization," *Nanoscale*, vol. 7, no. 3, pp. 1002–1012, 2015.

[35] S. K. Wirawan and D. Creaser, "CO_2 adsorption on silicalite-1 and cation exchanged ZSM-5 zeolites using a step change response method," *Microporous and Mesoporous Materials*, vol. 91, no. 1–3, pp. 196–205, 2006.

[36] X. Xu, X. Zhao, L. Sun, and X. Liu, "Adsorption separation of carbon dioxide, methane, and nitrogen on Hβ and Na-exchanged β-zeolite," *Journal of Natural Gas Chemistry*, vol. 17, no. 4, pp. 391–396, 2008.

[37] J. Ma, C. Si, Y. Li, and R. Li, "CO_2 adsorption on zeolite X/activated carbon composites," *Adsorption*, vol. 18, no. 5-6, pp. 503–510, 2012.

[38] T. F. d. Oliveira, E. S. Ribeiro, M. G. Segatelli, and C. R. T. Tarley, "Enhanced sorption of Mn^{2+} ions from aqueous medium by inserting protoporphyrin as a pendant group in poly(vinylpyridine) network," *Chemical Engineering Journal*, vol. 221, no. 2, pp. 275–282, 2013.

[39] Z. Zhao, X. Cui, J. Ma, and R. Li, "Adsorption of carbon dioxide on alkali-modified zeolite 13X adsorbents," *International Journal of Greenhouse Gas Control*, vol. 1, no. 3, pp. 355–359, 2007.

[40] X. Cui, R. M. Bustin, and G. Dipple, "Selective transport of CO_2, CH_4, and N_2 in coals: insights from modeling of experimental gas adsorption data," *Fuel*, vol. 83, no. 3, pp. 293–303, 2004.

[41] A. Perrin, A. Celzard, A. Albiniak, J. Kaczmarczyk, J. F. Marêché, and G. Furdin, "NaOH activation of anthracites: effect of temperature on pore textures and methane storage ability," *Carbon*, vol. 42, no. 14, pp. 2855–2866, 2004.

[42] M. M. Maroto-Valer, Y. Zhang, E. J. Granite, Z. Tang, and H. W. Pennline, "Effect of porous structure and surface functionality on the mercury capacity of a fly ash carbon and its activated sample," *Fuel*, vol. 84, no. 1, pp. 105–108, 2005.

[43] M. Gu, B. Zhang, Z. Qi et al., "Effects of pore structure of granular activated carbons on CH_4 enrichment from CH_4/N_2 by vacuum pressure swing adsorption," *Separation and Purification Technology*, vol. 146, pp. 213–218, 2015.

[44] S. Wang, L. Lu, D. Wu et al., "Molecular simulation study of the adsorption and diffusion of a mixture of CO_2/CH_4 in activated carbon: effect of textural properties and surface chemistry," *Journal of Chemical & Engineering Data*, vol. 61, pp. 4139–4147, 2016.

[45] J. Pokrzywinski, J. K. Keum, R. E. Ruther et al., "Unrivaled combination of surface area and pore volume in micelle-templated carbon for supercapacitor energy storage," *Journal of Materials Chemistry A*, vol. 5, no. 26, pp. 13511–13525, 2017.

[46] K. Munusamy, G. Sethia, D. V. Patil, P. B. Somayajulu Rallapalli, R. S. Somani, and H. C. Bajaj, "Sorption of carbon dioxide, methane, nitrogen and carbon monoxide on MIL-101(Cr): volumetric measurements and dynamic adsorption studies," *Chemical Engineering Journal*, vol. 195-196, no. 7, pp. 359–368, 2012.

[47] Y. Dang, L. Zhao, X. Lu et al., "Molecular simulation of CO_2/CH_4 adsorption in brown coal: effect of oxygen-, nitrogen-, and sulfur-containing functional groups," *Applied Surface Science*, vol. 423, pp. 33–42, 2017.

[48] W. Hao, F. Björnerbäck, Y. Trushkina et al., "WITHDRAWN: high-performance magnetic activated carbon from solid waste from lignin conversion processes. Part I: their use as adsorbents for CO_2," *Energy Procedia*, vol. 114, no. 12, pp. 6272–6296, 2017.

[49] W. Hao, E. Björkman, M. Lilliestråle, and N. Hedin, "Activated carbons prepared from hydrothermally carbonized waste biomass used as adsorbents for CO_2," *Applied Energy*, vol. 112, no. 3, pp. 526–532, 2013.